Innovative Dual-Excitation Drive in Fault Tolerant Double-Stator Vernier Machines for Ship Propulsion

Esmaeil Mohammadi
e-Motion Laboratory Department of Mechanical Engineering
University College London
London, UK
esmaeil.mohammadi.23@ucl.ac.uk

Ali Mohammadi
SPARK Lab, Department of Electrical and Computer Engineering
University of Kentucky
Lexington KY, USA
ali.mohammadi@ieee.org

Mohammad Amin Jalali Kondelaji
e-Motion Laboratory Department of Mechanical Engineering
University College London
London, UK
amin.jalali@ucl.ac.uk

Pedram Asef
e-Motion Laboratory Department of Mechanical Engineering
University College London
London, UK
pedram.asef@ucl.ac.uk

Dan M. Ionel
SPARK Lab, Department of Electrical and Computer Engineering
University of Kentucky
Lexington KY, USA
dan.ionel@ieee.org

***Abstract*—Electric propulsion has gained attention in the maritime industry due to its flexibility, energy efficiency, and adaptability for diverse ship types, including icebreakers, cruise ships, and research vessels. The continuous advancement of motor technologies has significantly redefined propulsion systems. Among these innovations, axial flux permanent magnet synchronous machines (AFPMSMs) stand out for their exceptional torque density, making them particularly suitable for low-speed direct-drive applications. Additionally, the high torque at low rotational speeds of the machine contributes to streamlining drivetrain complexity and reducing maintenance demands. This paper introduces a novel 1 MW AFPMSM, MAGNUS, which combines an inner spoke-rotor with dual external high-polarity stators with a minimal number of teeth, capable of operating with a single stator during faulty conditions. Performance indices for traction applications, derived from analytical torque-speed characteristics and Finite Element Analysis (FEA) calculated torque versus torque angle, demonstrate the effectiveness of the proposed machine architecture. These results indicate the machine's capability to maintain operation within the constant power region of its torque-speed profile. In faulty scenarios, its dual-stator configuration and independent drives ensure approximately 70% torque retention, supporting safe and reliable marine operation. Furthermore, the compact and thermally robust structure accommodates scalable power levels, making it a compelling solution across a wide range of vessel classes.**

***Keywords*—Axial flux motors, electric propulsion, fault tolerance, flux weakening, ship propulsion, spoke rotor.**

I. Introduction

Ship propulsion systems represent a critical domain of maritime engineering, continually evolving to meet the growing demands for efficiency, reliability, and environmental sustainability. Traditional propulsion technologies, while effective, often face challenges in adapting to modern requirements for operational flexibility, reduced emissions, and cost efficiency. In this context, electric propulsion has emerged as a transformative solution, leveraging advancements in motor technologies to redefine maritime operations. Ship propulsion operates at relatively low speeds, with shaft speeds typically ranging between 100 and 500rpm for large vessels. High torque production at low rotational speeds eliminates the need for a mechanical gear reduction system, simplifying the propulsion setup while reducing maintenance requirements. This streamlined design enhances overall reliability and operational efficiency. Among the innovative solutions under development, axial flux permanent magnet (AFPM) motors have gained significant attention due to their exceptional torque density, compact structure, and Effectiveness in operating in low-speed, high-torque applications [1]-[4].

Direct-drive permanent magnet (PM) motors appear to be the most promising solution that achieves the requirements of the marine industry, especially in terms of high efficiency and reliability. Additionally, the compactness and high torque density of direct-drive PM motors make them particularly suitable for integration into constrained marine environments, where spatial and weight limitations are critical considerations. These characteristics, combined with superior dynamic performance and precise controllability, render them highly attractive for modern electric ship propulsion systems that prioritise operational stability and sustainability [5], [6].

Recent developments in axial flux motor topologies have shown promising potential for marine propulsion applications, particularly in rim-driven thruster systems. AFPM machines have many advantages like superior magnetic performance, high torque density, operational flexibility and a unique stator design which facilitates the integration of advanced cooling systems, including micro-channels embedded within the slots [7]. These micro-channels enable efficient cooling by allowing for increased current density in the stator windings without compromising thermal limits. Furthermore, for electric motors with high torque density used in ship propulsion, effective cooling systems are essential to maintain ideal operating temperatures and ensure sustained reliability and performance. In this context, the Axial Flux Motor (AFM) constitutes a promising alternative due to its compact structure and effective thermal characteristics. Additionally, the motor's compact design and scalable architecture make AFPMSM suitable for a wide range of ship applications [8], [9].

An analysis was conducted on a double-stator, ironless rotor AFPM machine, introducing a three-dimensional analytical magnetic model that incorporates image theory and permeance functions to account for stator slotting, alongside a simplified thermal model to assess loss sensitivity and cooling capacity. To reduce material costs, a genetic algorithm was employed under multiple electrical,

geometrical, and mechanical constraints, yielding superior performance in cost and weight compared to a reference radial flux PM machine [10].

In parallel, a novel ring-winding AFM topology was proposed, offering structural simplicity, high reliability, and scalability in phase and pole count key attributes for marine systems. This design approach explicitly considers the close coupling between electromagnetic performance and the propeller–hull geometry, underscoring the suitability of ring-winding AFMs for integrated marine propulsion systems [11]. Another investigation introduced axial field machines with a high rotor pole to stator tooth ratio for low-speed direct-drive traction. Featuring spoke-type PM and auxiliary stator slots, the design improves torque production. Multiple phase configurations, including biphasic and triphasic systems, offer inherent fault tolerance and improved performance over traditional PM synchronous machines. Additionally, AFPM machines, capable of operating efficiently at low speed, which serves as a suitable substitute for conventional motors [12], [13].

This paper explores a novel 1 MW AFPMSM motor topology specifically designed for ship propulsion, featuring two active stators with unique dual-mode operational capability. This innovative AFPMSM motor topology presents a promising step forward in the evolution of maritime propulsion systems. By integrating design principles and addressing critical industry challenges, it has the potential to redefine the standards for efficiency, reliability, and sustainability in the maritime sector. The remainder of this paper is structured in four sections. Section II presents the detailed design methodology of the proposed machine. Section III evaluates its performance under both normal operating conditions and fault scenarios, with the results compared in a dedicated table to demonstrate the machine's robustness and consistency. Section IV concludes the paper by summarising the key findings and contributions.

II. Methodology

The electric machine discussed in this paper, as illustrated in Fig. 1, is designed with dual stators, each comprising 36 teeth with split poles. These stators are structured to include three-phase windings, with 36 coils arranged in a double-layer configuration on the teeth. To enhance performance and minimise electromagnetic interference, one stator is positioned with an axial rotational offset of 0.5 electrical degrees relative to the other. This strategic displacement enhanced magnetic coupling, contributing to improved operational efficiency and fault tolerance. The operational principle of the MAGNUS machine relies on the modulation of the armature magnetomotive force (MMF) to create a flux density component within the air gap that aligns with the rotor poles. This modulation is facilitated through the use of stators' teeth and slots, which are designed with a pole configuration that differs from that of the rotor. A specific relationship exists between the number of rotor poles, the teeth on the main and auxiliary stators, and the armature poles to achieve this functionality.

To determine the required number of rotor poles for a three-phase configuration, two key conditions must be met. Firstly, there should be an odd number of PM poles facing each stator tooth to ensure that only poles of one polarity contribute to the phase flux linkage at any given time. Secondly, a 120-degree phase shift is necessary between the phases. For the motor under consideration, the stators are designed with 36 teeth, resulting in a configuration with 120 rotor poles that satisfies the required design criteria. The rotor, equipped with 120 PMs in a spoke-type configuration, achieves high flux concentration and has been systematically analysed at various positions along the radial direction within the machine's air gaps. The specific relationship between the number of rotor poles, main and auxiliary stator teeth, and armature poles is established as:

$$P_r = 2 \times T_{ms} \times t_{st} - P_a, \tag{1}$$

where P_r is the number of rotor poles, which is equal to 120, T_{ms} the number of stator main teeth, which is 36, t_{st} the number of auxiliary stator teeth, which is 2, and P_a the number of armature poles is 24 in this design.

The proposed machine is powered by two separate and independent advanced power electronic drives, as shown in Fig. 1. Each of which operates an individual stator under nominal current density. This independent control mechanism ensures precise regulation of motor functions, optimising both performance and fault tolerance [14], [15]. During fault conditions, the affected stator assumes a passive role, while the active stator receives double the rated current density (2×5A/mm²) from the corresponding drive. The drives are equipped with completely independent circuits and are designed to provide double the current density to the circuit, ensuring enhanced performance and reliability under high-current operating conditions. This process is effectively managed by integrating an advanced cooling system, which ensures thermal stability and prevents overheating, thereby enhancing the machine's reliability and efficiency. A key

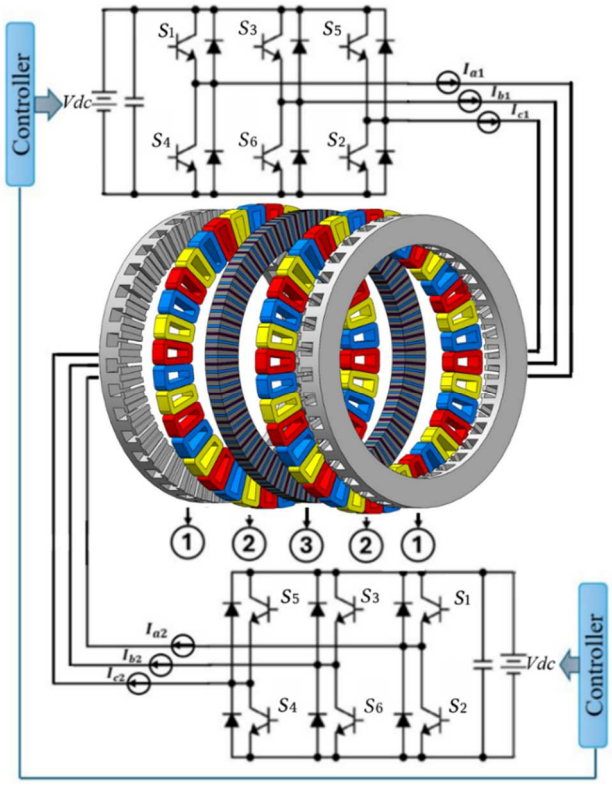

Fig. 1. Machines 3D exploded view with drives and controllers. (1) Stators. (2) Three phase coils. (3) Common rotor.

advantage of the proposed topology is its ability to maintain operational continuity in the event of a fault in one of the stators, in contrast to conventional radial motors, which become non-functional under similar fault conditions.

This adjustment enables the machine to generate approximately 70% of its nominal torque, even under non-ideal conditions. Such a capability is critical in high-stakes applications like ship propulsion, where uninterrupted performance is not only desirable but often essential to the safety and reliability of operations. This innovative dual-stator machine is an exemplary choice for high-reliability applications like ship propulsion, addressing the maritime industry's demands for dependability, efficiency, and adaptability while extending system longevity and showcasing the promise of innovative engineering solutions.

The torque generated by the machine can be determined by leveraging its unique structural design and operational principles. The combination of these stators, with their specifically designed teeth and slots, aligns the flux density within the air gap to interact effectively with the rotor poles. The spoke-type rotor ensures high flux concentration, further amplifying the torque output which can be obtained by:

$$T_{em} = \frac{\partial W_{co}}{\partial \theta_r} = \frac{\partial}{\partial \theta_r} \int \frac{B(\emptyset,t)^2}{2\mu} dv, \tag{2}$$

$$\frac{D_r g L_{stk}}{4\mu} \frac{\partial}{\partial \theta_r} \int_0^{2\pi} (B_{PM}(\phi,t) + B_R(\phi,t)^2 d\emptyset, \tag{3}$$

where D_r is the average diameter, g is the air-gap, and L_{stk} is the radial stack length.

In AFPM machines, the air-gap flux density has two main components, one in the axial direction and the other in the tangential direction. These two components of the air gap flux density distribution at an arbitrary rotor position are obtained from 3-D FEA. The air-gap flux density can be decomposed into a series of harmonics. With the air-gap flux density harmonics, the torque contributed by each harmonic is:

$$T = \sum_k \left(\frac{D_r}{2}\right)^2 L_{stk} |B_a^k| |B_t^k| \cos(\theta_a^k - \theta_a^k), \tag{4}$$

TABLE I. PARAMETERS AND SPECIFICATIONS

Parameter	Value
Rated power	1MW
Rotor outer diameter	1500mm
Rotor inner diameter	1200mm
Number of rotor poles	120
Axial length	400mm
Rated speed	300rpm
Number of turns per coil	50
Rated current density	5A/mm^2
Air-gap length	1.5mm

where D_r represents the average diameter of the rotor, L_{stk} denotes the radial stack length of the rotor, k is the harmonic number, B_a and B_t correspond to the axial and tangential components of flux density in the air-gap, respectively.

The tangential force acting on individual stator teeth and rotor components can be determined by integrating the stress across the corresponding mechanical elements such as:

$$F_t = \int f_t(t,\theta) ds. \tag{5}$$

III. Results and Discussion

Due to the substantial size of the full model, 3D FEA simulations are conducted on 1/12 of the complete structure, taking advantage of the electromagnetic symmetry of the topology. The machine's meshing model and the flux density distributions are illustrated in Fig. 2 (a) and (b), respectively. The number of mesh elements is approximately one million. In the proposed machines, the flux density exceeds 2T in the spoke rotor and in the stators, demonstrating their ability to handle high magnetic loads efficiently. The auxiliary teeth also experience a notably higher flux density, further contributing to the machine's magnetic performance.

In contrast, the back iron of the stators is subjected to significantly lower flux density, ensuring a balanced magnetic distribution and effective utilisation of the magnetic circuit components. Moreover, the auxiliary teeth experience saturation levels comparable to those in the spoke-type configuration. Consequently, ensuring sufficient core thickness during the design phase is crucial to diminishing excessive magnetic saturation and maintaining optimal performance.

Fig. 3 (a) illustrates the faulted model, in which one of the stators experiences a fault; in this mode, the affected stator operates as a passive stator. Fig. 3 (b) indicates that the

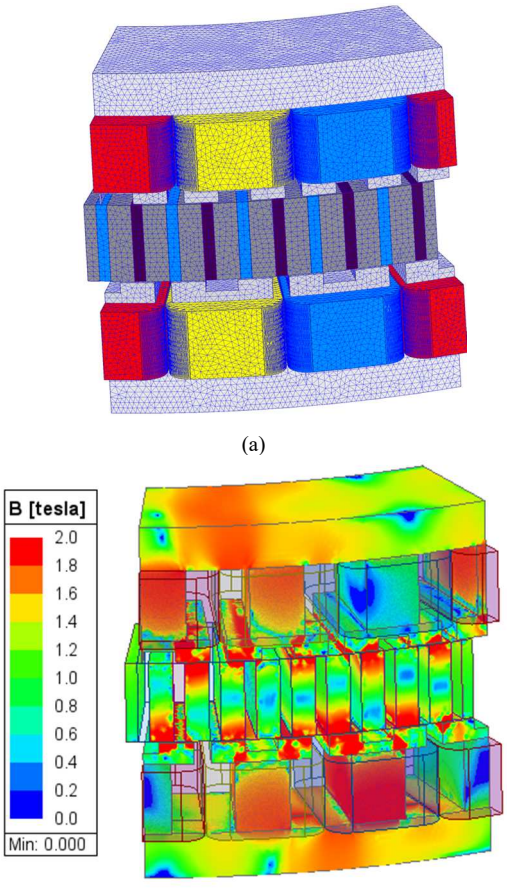

(a)

(b)

Fig. 2. (a) Tetrahedral mesh elements. (b) Magnetic flux density of the model.

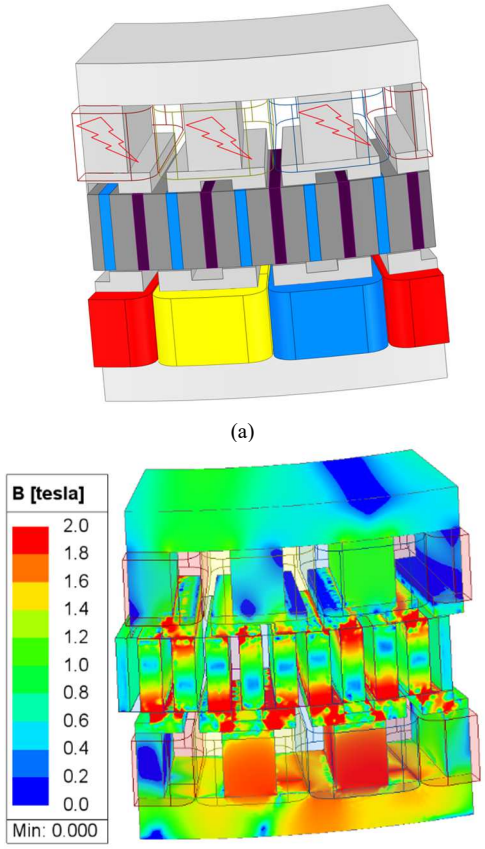

(a)

(b)

Fig. 3. (a) Faulted model (one active and one passive stator). (b) Magnetic flux density of the faulted model.

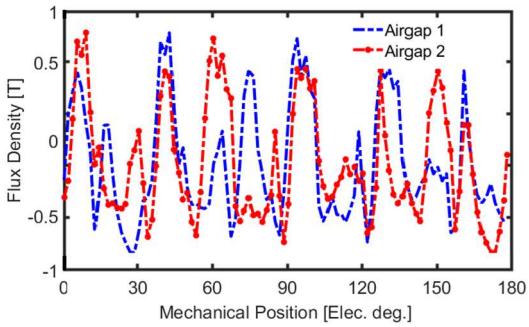

Fig. 4. The flux density of the airgaps.

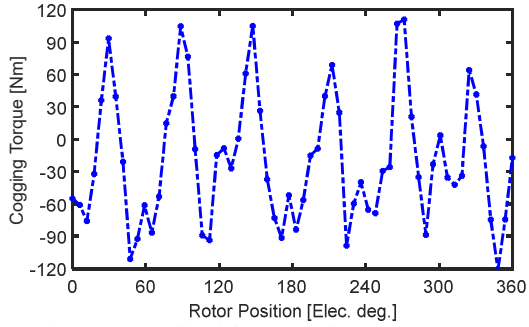

Fig. 5. Cogging torque profile of the proposed motor.

flux density surpasses 2T while the fault-free stator receives twice the rated current density, indicating their robust capability to sustain elevated magnetic loading with a high efficiency of 92.8%. Additionally, the auxiliary teeth exhibit a significantly intensified magnetic flux, which further enhances the overall electromagnetic performance of the machine.

Fig. 4 illustrates the airgaps flux density distribution for the proposed machine and highlights how the flux density varies across the airgaps, providing valuable insights into the magnetic field characteristics and performance of the machine. A well-distributed and symmetric flux pattern indicates efficient magnetic circuit utilisation and reduced core saturation. Analysing these variations helps assess potential regions of flux concentration, which are critical for thermal management and minimising local electromagnetic losses.

The waveforms of cogging torque for the machine configuration, as shown in Fig. 5, indicate that the spoke-type machine exhibits a cogging torque of 200Nm peak-to-peak. Considering the motor's size and its rated torque of 32kNm, this corresponds to only 0.625%, which is relatively low and highlights the effectiveness of the machine's design in minimising cogging torque. This reduction is likely attributed to optimised rotor pole geometry and slot-pole combinations that disrupt periodic magnetic attraction. Reducing cogging torque not only enhances mechanical smoothness but also contributes to reduced acoustic noise and improved control precision at low speeds.

Fig. 6 demonstrates that the proposed model attains a peak-to-peak flux linkage of approximately 0.8Wb. This elevated flux linkage reflects effective magnetic coupling between stator and rotor components, indicating strong utilisation of the magnetic circuit.

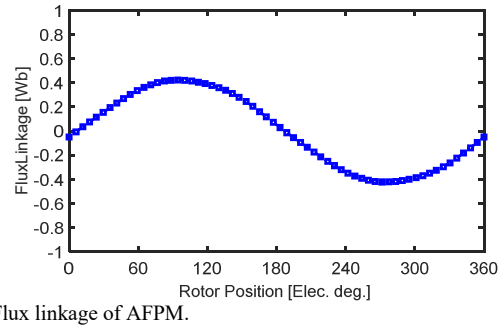

Fig. 6. Flux linkage of AFPM.

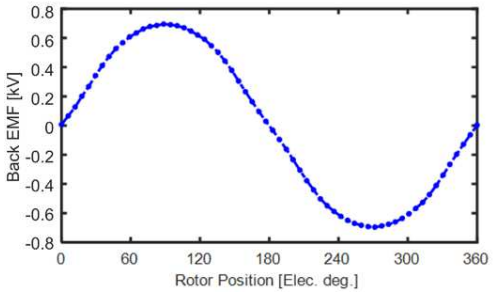

Fig. 7. Back-EMF waveform at the rated speed.

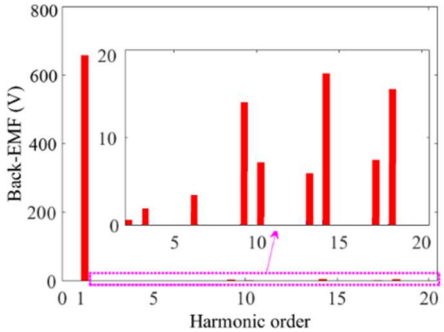

Fig. 8 Harmonic spectra of the back-EMF waveform.

TABLE II. COMPARATIVE PERFORMANCE EVALUATION OF THE MACHINE UNDER HEALTHY AND UNHEALTHY CONDITIONS

Design Condition	J (A/mm²)	Emag. Torque (kNm)	T-Ripple (%)	Power (kW)	Efficiency (%)	Kt (Nm/(A/mm²))	Torque Density (Nm/L)
Healthy	5	32	3	1000	95	6400	126
Unhealthy	10	22	4	700	92.8	2200	88

The pronounced flux concentration arises from optimised geometric design and material selection, enhancing the machine's ability to generate electromagnetic torque. As a result, the model exhibits improved overall performance and energy conversion efficiency.

Harmonic components may excite mechanical resonances, intensifying vibration and acoustic emissions. Consequently, detailed harmonic analysis of the BEMF is critical to achieving reliable and efficient machine operation. Fig. 7 illustrates the back electromotive force (BEMF) waveform of the machine, reaching peak amplitude of 650V. Magnitude of harmonic components, as illustrated in Fig. 8. These harmonics contribute to a total harmonic distortion (THD) of 4%, which can induce torque ripple, elevate core and copper losses, and complicate control strategies. The amplitudes of the higher-order harmonics are relatively low, indicating a reduced THD and, consequently, a lower expected torque ripple.

Fig. 9 shows that at a current density of 5A/mm² for both active stators, the machine delivers a torque output of 32kNm with a torque ripple of 3%. In scenarios where one of the stators becomes inactive, either due to a fault or for servicing, the independent converters ensure continuous operation by injecting twice the current into the remaining active stator.

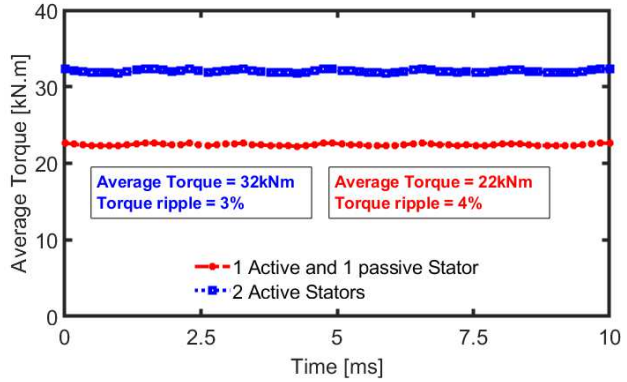

Fig. 9. Torque for the topologies in normal and fault conditions.

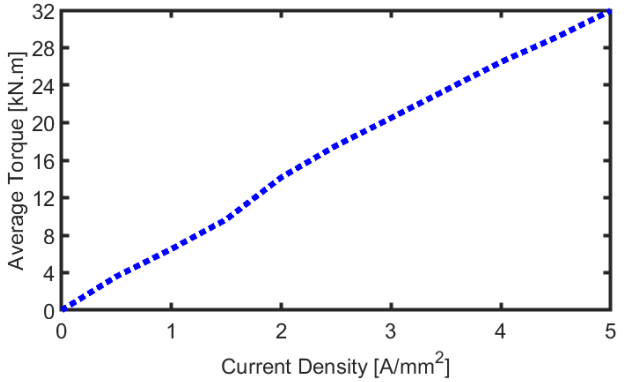

Fig. 10. Torque versus current density.

This adjustment is made possible with the implementation of an advanced cooling system, ensuring efficient heat dissipation. As a result, the active stator can generate approximately 70% of the total torque, which is 22kNm, maintaining significant machine performance despite the inactive stator with a slightly elevated torque ripple of 4%.

The relationship between torque and current density for the model shown in Fig. 10 demonstrates a nearly linear increase as the current density rises. This trend emphasises the model's efficiency in converting electrical energy into mechanical torque. The linear behaviour indicates that the torque output remains consistent and predictable over a range of current densities, making it a valuable characteristic for performance optimisation and reliable machine operation.

Table II presents a comparative performance analysis of the motor under both healthy and faulty operating conditions, demonstrating the system's robustness and resilience. Despite the increase in current density from 5A/mm² to 10A/mm² under unhealthy conditions, the motor maintains continuous operation without thermal or electrical failure, attributable to the implementation of advanced cooling strategies. Remarkably, even with one active stator under faulty conditions, the motor continues to deliver substantial torque, decreasing from 32kNm to 22kNm, yet still ensuring reliable mechanical propulsion for mission-critical marine operations. The power output remains within acceptable thresholds, reducing from 1000kW to 700kW, with only a marginal efficiency drop from 95% to 92.8%. Notably, this demonstrates that the system sustains operation at approximately 70% of its nominal power. Furthermore, the torque constant (Kt) remains well preserved under faulted conditions, underscoring the consistency of the machine's electromagnetic behaviour and reinforcing the fault-tolerant capability of the proposed design.

IV. Conclusion

This paper introduced a 1 MW axial flux permanent magnet synchronous machine (AFPMSM) for a direct-drive marine electric propulsion system. The proposed design integrated an inner spoke-type rotor with dual high-polarity stators, resulting in compact dimensions, high torque density, and simplified drivetrain integration. The machine's performance across a broad torque-speed operating range was analysed using 3-D finite element analysis (FEA) and demonstrated its ability to meet the operational demands of modern electric ships. The motor exhibited strong fault-tolerant behaviour. Under healthy conditions, it delivered 32kNm of torque with a torque ripple of 3% and achieved an efficiency of 95%. In the faulty scenarios, the independent drive system supplied the active stator with double the rated current density, which was mitigated by an advanced cooling strategy. The faulty stator operated as a passive component, and the motor continued to deliver 22kNm of torque with a torque ripple of 4%, while maintaining an efficiency of

92.8%. This performance, corresponding to approximately 70% of its nominal power, ensured uninterrupted propulsion and confirmed the reliability of the proposed design under degraded conditions. Overall, the MAGNUS motor offered a scalable and reliable solution for sustainable marine propulsion, combining performance continuity with structural and thermal integrity. Its architecture held strong potential for integration into future electric ship platforms where efficiency, reliability, and maintainability are paramount.

REFERENCES

[1] A. Mohammadi, Y. Chulaee, A. M. Cramer, I. G. Boldea and D. M. Ionel, "Large-Scale Design Optimization of an Axial-Flux Vernier Machine With Dual Stator and Spoke PM Rotor for EV In-Wheel Traction," in *IEEE Transactions on Transportation Electrification*, vol. 11, no. 1, pp. 2477-2488, Feb. 2025, doi: 10.1109/TTE.2024.3423713.

[2] O. Dobzhanskyi and E. Amiri, "Performance Analysis of the Transverse-Flux Machine with High number of Poles for Large Wind, Hydro, and Electric Ship Propulsion Systems," *2020 IEEE Green Technologies Conference(GreenTech)*, Oklahoma City, OK, USA, 2020, pp. 1-6, doi: 10.1109/GreenTech46478.2020.9289813.

[3] J. L. Kirtley, A. Banerjee and S. Englebretson, "Motors for Ship Propulsion," in *Proceedings of the IEEE*, vol. 103, no. 12, pp. 2320-2332, Dec. 2015, doi: 10.1109/JPROC.2015.2487044.

[4] H. Zhao, C. Liu, Z. Dong, R. Huang and X. Li, "Design and Optimization of a Magnetic-Geared Direct-Drive Machine With V-Shaped Permanent Magnets for Ship Propulsion," in *IEEE Transactions on Transportation Electrification*, vol. 8, no. 2, pp. 1619-1633, June 2022, doi: 10.1109/TTE.2021.3124891.

[5] N. Arish, M. J. Kamper and R. -J. Wang, "Optimization and Comparative Analysis of Magnet Shapes in 5-MW PM Vernier Motors for Marine Propulsion," *2024 International Conference on Electrical Machines (ICEM)*, Torino, Italy, 2024, pp. 1-7, doi: 10.1109/ICEM60801.2024.10700532.

[6] J. Yu, W. Mi, Z. Cai, Z. Song, S. Liu and C. Liu, "Design Principle Considering Structural Mutual Effects of Double-Stator V-Shape-PM Vernier Machines for Electric Ship Propulsion," in *IEEE Transactions on Transportation Electrification*, vol. 10, no. 1, pp. 496-508, March 2024, doi: 10.1109/TTE.2023.3279202.

[7] L. Wu and Z. Tian, "Analysis of a Triple-Stator Axial-Flux Spoke-Type Permanent Magnet Vernier Machine," in *IEEE Transactions on Industry Applications*, vol. 58, no. 5, pp. 6024-6034, Sept.-Oct. 2022, doi: 10.1109/TIA.2022.3178686.

[8] R. Roy, S. Ramasami and L. N. Chokkalingam, "Review on Thermal Behavior and Cooling Aspects of Axial Flux Permanent Magnet Motors–A Mechanical Approach," in *IEEE Access*, vol. 11, pp. 6822-6836, 2023, doi: 10.1109/ACCESS.2023.3235782.

[9] G. Cakal and B. Sarlioglu, "Review of Advances in Cooling Schemes for Yokeless and Segmented Armature (YASA) Axial Flux Motors," *2023 25th European Conference on Power Electronics and Applications (EPE'23 ECCE Europe)*, Aalborg, Denmark, 2023, pp. 1-8, doi: 10.23919/EPE23ECCEEurope58414.2023.10264667.

[10] Ouldhamrane, H., Charpentier, J.-F., Khoucha, F., Zaoui, A., Achour, Y., and Benbouzid, M., "Optimal design of axial flux permanent magnet motors for ship RIM-driven thruster," *Machines*, vol. 10, no. 10, p. 932, 2022, doi: 10.3390/machines10100932.

[11] P. Ojaghlu and A. Vahedi, "Specification and Design of Ring Winding Axial Flux Motor for Rim-Driven Thruster of Ship Electric Propulsion," in *IEEE Transactions on Vehicular Technology*, vol. 68, no. 2, pp. 1318-1326, Feb. 2019, doi: 10.1109/TVT.2018.2888841.

[12] V. Rallabandi, P. Han, M. G. Kesgin, N. Taran and D. M. Ionel, "Axial-field Vernier-type Flux Modulation Machines for Low-speed Direct-drive Applications," *2019 IEEE Energy Conversion Congress and Exposition (ECCE),* Baltimore, MD, USA, 2019, pp. 3123-3128, doi: 10.1109/ECCE.2019.8912550.

[13] M. Vatani, D. R. Stewart, P. Asef, and D. M. Ionel, "Optimal Design of Coreless Axial Flux PM Machines Using a Hybrid Machine Learning and Differential Evolution Method," *IEEE International Electric Machines and Drives Conference (IEMDC),* Houston, USA, 2025, pp. 1-6.

[14] F. Perabo and M. Zadeh, "Multiphysics Modelling and Co-Simulation of Ship Electric Power and Propulsion Systems for Virtual Testing and Verification," in *IEEE Transactions on Transportation Electrification*, vol. 11, no. 1, pp. 5108-5121, Feb. 2025, doi: 10.1109/TTE.2024.3480009.

[15] S. Ni, C. Li and Z. Zheng, "Control Strategy of a Hybrid SiC-Si Traction Inverter for Direct-Drive Multiphase PMSMs in Marine Propulsion," in *IEEE Transactions on Power Electronics*, vol. 39, no. 12, pp. 16400-16414, Dec. 2024, doi: 10.1109/TPEL.2024.3434703.